Within-field advection enhances evaporation and transpiration in a vineyard in an arid environment

Dilia Kool[a], Alon Ben-Gal[b], Nurit Agam[a],*

[a] Blaustein Institutes for Desert Research, Ben-Gurion University of the Negev, Israel
[b] Gilat Research Center, Agricultural Research Organization, Israel

ARTICLE INFO

ABSTRACT

Advection of hot air from a warmer to a cooler surface is known to enhance evaporation through additional supply of energy, provided that water is readily available. This study investigated advection in an isolated irrigated vineyard in the Negev desert, over a period of several months under changing plant cover and environmental conditions, and for different degrees of water availability. Field, canopy, and soil energy balance fluxes were assessed, as well as likely indicators of advection such as wind speed, VPD, vertical temperature gradients between the soil, the canopy air space, and the air, and lateral temperature gradients between the vineyard and the surrounding desert. It was found that for a period from May to July, advection enhanced transpiration by 8%, where diurnal patterns suggested that most of the advection originated from within the field. At times, soil-to-canopy advection enhanced transpiration by as much as 30–40%. Wet irrigated strips likewise experienced soil-to-soil advection from drier soil, but to a much lesser degree. A surprisingly large difference was observed in the contribution of advection to transpiration between June (2%) and July (11%), which had almost identical environmental conditions. This indicates that small changes in the agro-system such as row-width and leaf area could have a large impact on within-field advection, and that row crops could potentially be managed to reduce or enhance advection.

1. Introduction

Water use in arid environments is dictated by evapotranspiration, including evaporation from the soil and plant transpiration. Evapotranspiration and its partitioning determines plant growth, ecosystem functioning, and weather patterns; and better quantification of its drivers can help improve irrigation practices, prevent desertification, and improve climate models. Net radiation (R_n) is the primary source of energy for evapotranspiration, or latent heat flux (LE), but advection of heat energy can also be a major contributor under certain conditions.

In applied meteorology, this type of advection is defined as net horizontal transport of sensible heat (H) between a field and its surroundings; where horizontal transport generally occurs in a downwind direction, through wind sweeping over and through a field (McNaughton and Jarvis, 1983; Oke, 1987; Prueger et al., 1996; Hillel, 1998). Advected sensible heat adds available energy to a field when the field is cooler than its surrounding, as is often the case for irrigated areas or oases (Tolk et al., 2006; Díaz-Espejo et al., 2008). This additional energy can enhance LE when available energy is the limiting factor for evapotranspiration, either because of high demand, i.e. when

soil water supply and evaporative demand are high and plants are physically capable of transpiring more (McNaughton and Jarvis, 1983; Oke, 1987; Yunusa et al., 2004); or because of low available energy, e.g. at night, when advection can cause night time transpiration (Hanks et al., 1971). Other types of advection, such as the advection of vapor pressure deficit (VPD) or 'dry air', which may enhance evaporation and affect the energy balance by horizontal transport of latent heat (Slatyer and McIlroy, 1961; McNaughton, 1976; Monteith, 1981). The primary focus of this paper is sensible heat advection; thus, unless otherwise specified, advection in this paper refers to conditions where advected H enhances LE.

Advection can be quantified as $-H$, or $LE - R_n - G < 0$, where R_n is net radiation, G is soil heat flux, and defining R_n as positive towards the surface and LE, H, and G as positive away from the surface. This approach may underestimate advection, as studies have shown that advection can sometimes be larger than the downwelling heat flux, due to the importance of turbulence in transporting energy fluxes (Zermeño-Gonzalez and Hipps, 1997; Prueger et al., 2012). While this is the most common way to quantify advection (Ham et al., 1991; Heilman et al., 1994; Prueger et al., 1996; Daamen, 1997; Lund and

---

Soegaard, 2003; Alfieri et al., 2012), alternative ways include comparing *LE* to equilibrium *LE (LE$_{eq}$)*, defined as the equilibrium evaporation rate over a saturated surface (Priestley and Taylor, 1972), formulated as:

$$LE_{\text{eq.}} = \frac{s(R_n - G)}{s + \gamma} \tag{1}$$

where *s* is the slope of saturated vapor pressure vs. temperature and γ is the psychrometric constant. The ratio $LE/LE_{\text{eq.}}$, known as the Priestley-Taylor coefficient (α_{PT}; Priestley and Taylor, 1972), equals one if both the surface and the air are saturated. However, in the absence of advection, α_{PT} typically equals approximately 1.26 (Eichinger et al., 1996). Thus, advection over wet surfaces has also been defined as $\alpha_{PT} > 1.26$ (Diaz-Espejo et al., 2005). However, in some cases *H* does not turn negative until α_{PT} reaches 1.4 or 1.5 (Diaz-Espejo et al., 2005; Li and Yu, 2007). The first difficulty with defining advection as $\alpha_{PT} > 1.26$ is that this threshold is only valid for well-watered conditions, while advection may also occur under drier conditions so long as energy is limiting evaporation. Secondly, the 1.26 value, though reported to be valid under a range of conditions, is empirical and somewhat arbitrary. It appears therefore that −*H* is the most straightforward way to quantify advection, with the understanding that advection might be larger than −*H*, while the more empirical $\alpha_{PT} > 1.26$ can serve as an indicator of advection under well-watered conditions.

Advection is commonly specified to be "regional" or "local" referring to the assumed source of advected *H* (Brakke et al., 1978; Tolk et al., 2006). Regional advection is thought to occur on a scale > 1 km (Prueger et al., 2012), or even > 100 km (Ringgaard et al., 2014), and will affect an entire irrigated area. Local advection originates from adjacent drier and warmer areas and will most strongly enhance evaporation in the upwind section of the field, with declining influence on evaporation as the horizontally moving air comes into equilibrium with the surface (Brakke et al., 1978; Tolk et al., 2006). Thus, regional and local advection are often distinguished using measurements of *H* close to the edge and in the middle of a large field, where the contribution of regional advection is equal to −*H* in the middle of the field and local advection is considered the source for any additional −*H* near the edge (Brakke et al., 1978). However, Zermeño-Gonzalez and Hipps (1997) postulated that the assumed decline of the influence of local advection on *H* in a downwind direction may not always be correct for vegetated surfaces. The increase in transpiration in the upwind section of the field may decrease the vapor pressure deficit further downwind. This could reduce stomatal resistance in the downwind area, enhancing transpiration indirectly. Prueger et al. (2012) noted that spectral analysis of the turbulence structure in the surface boundary layer during advective conditions may shed some light on the origins of advection, e.g. the variance in temperature caused by larger eddies are likely to originate from further away. However, much of the turbulent processes during advective conditions are still not fully understood. Determining whether advection is regional or local and quantifying advection in general is therefore not straight-forward.

In addition to regional and local advection, in ecosystems with partial canopy cover, such as row-crops, orchards, or shrublands, distinct dry and wet zones within a field can cause within-field advection, occurring at a much smaller scale. Unlike regional or local advection, within-field advection is not driven by wind. Rather, free convection from a dry (warmer) surface is drawn in circular motions to wet (cooler) surfaces (Graser et al., 1987). Within-field advection tends to occur in semi-arid and arid environments, where temperature gradients between drier and wetter surfaces are more pronounced (Lund and Soegaard, 2003). The most common form of within-field advection is from a dry exposed soil surface to a wetter vegetated surface (soil-to-canopy advection). This type of advection has been referred to as within-canopy advection (Hanks et al., 1971), inter- or within row advection (Graser et al., 1987; McGowan et al., 1991; Heilman et al., 1994; Lund and Soegaard, 2003), convection (Figuerola and Berliner,

2006) or simply horizontal heat flux between the soil and the plant (Blyth and Harding, 1995). Advection from a dry canopy to a wet soil (canopy-to-soil advection) can occur when soil water evaporation is the main component of evapotranspiration, and has also been referred to as within row advection (Ham et al., 1991). A third form of within-field advection is heat transfer below the canopy, from drier to wetter parts of the soil surface (soil-to-soil advection). This type of advection has been referred to as micro or micro-scale advection and has been studied in drip-irrigated fields (Bonachela et al., 2001; Yuge et al., 2005, 2014; Figuerola et al., 2013).

For canopies with partial cover, not only is within-field advection more likely to occur, but there is also a decreased likelihood of local advection, because hot dry surfaces within the field decrease the temperature gradient between the field and its surroundings (Stoughton et al., 2002). In irrigated cotton, for example, it was observed that local advection was minimal at early stages of canopy growth, but increased as the canopy increased (Alfieri et al., 2012). Under within-field advective conditions, *H* from a wet surface within the field is negative but the average *H* for the field (*H$_{field}$*) can be positive or negative. Negative *H$_{field}$* and canopy *H* (*H$_c$*) were observed in sprinkler irrigated cotton in Texas, where negative *H$_{field}$* was considered local advection, and the remaining negative *H$_c$* was considered within-field advection, accounting for 21% and 12% of transpiration respectively (Ham et al., 1991). In a flood irrigated vineyard in Texas 17–36% of transpiration was attributed to advection, and, as no negative *H$_{field}$* was observed, all advection was assumed to have been generated within the field (Heilman et al., 1994). A different strategy has been applied to determine within-field advection from dry to wet soil, where advection was estimated as the surplus of *LE* from a wet soil surface within a field with intermittent wet and dry surfaces relative to the theoretical *LE* of a homogeneously wetted soil surface (Bonachela et al., 2001).

A better understanding of both the magnitude and the source of advection is required to measure or model evapotranspiration components in semi-arid and arid regions. Depending on the source of advection, energy balance models have to allow energy exchange between wetter and drier surfaces within the field or consider sources outside the field may contribute to available energy. There is also evidence that advection decreases the efficiency of plant carbon uptake per unit of water used (McGowan et al., 1991; Li and Yu, 2007). Specifically within-field advection was found to negatively affect water use in a field, where plants growing in widely spaced rows transpired more water per unit ground cover while producing less dry biomass than their narrow row counterparts (McGowan et al., 1991). A better understanding of advection may help determine if management strategies such as row spacing could be adapted to reduce these negative effects.

Great advancements have been made in studying different kinds of advection, including detailed measurements of a grid of irrigated and dry lysimeters (Diaz-Espejo et al., 2005), and comprehensive short-term measurements in the field (e.g. Ham et al., 1991). The limitations of these short-term measurements is that they neither incorporate changes in advective conditions as a function of evaporative demand and plant cover (Diaz-Espejo et al., 2005; Bonachela et al., 2012), nor account for effects of irrigation and plant drought stress (Ham et al., 1991; Gutiérrez and Meinzer, 1994). Seasonal studies have used combined measurement and modeling efforts (e.g. Lund and Soegaard, 2003) but we are unaware of any seasonal assessment of advection using independent estimation of soil and plant energy balance components.

The aim of this study is to assess the contribution of advection to soil and plant energy balance components in a drip-irrigated vineyard in an arid environment, and evaluate changes in advective conditions with canopy growth, evaporative demand, and irrigation.

2. Methods

2.1. Site description

Data were collected as part of a larger experiment in a commercial drip-irrigated vineyard in the arid Negev Highlands in Israel (30.7°N, 34.8°E) in the year 2012. The vines, *cv.* Cabernet-Sauvignon (*Vitis vinifera* L.), were trained on a vertical shoot-positioned system, with 1 m spacing between vines and 3 m spacing between the north-south oriented rows. The cordon height was 1 m, and at maturity the 10-year-old vines were about 1.8 m high and 0.5 m wide. The isolated ~10 ha vineyard was set on a level terrain, surrounded by desert. Long-term average minimum and maximum temperatures are 4.4 °C and 14.8 °C respectively in January, and 18.1 °C and 32.7 °C in July; precipitation (< 100 mm y^{-1}) is erratic and limited to the winter months (Israel Meteorological Service). Cumulative rainfall during the winter of 2011/2012 amounted to 48.3 mm, where the last rain event of 2.5 mm occurred on 16 March. No rainfall occurred during the growing season of 2012, which started with bud-break on 1 April.

2.2. Experimental set-up

Measurements were conducted from April 1 to July 25, ending just prior to harvest in early August. A micrometeorological station was set up at a distance of about 300 m from the edge of the field in the pre-vailing wind direction (NW), with a fetch of about 150 m in all other directions (Fig. 1). The instrumentation and micrometeorological conditions at the site have been described in detail by Kool et al. (2014, 2016). In brief, the standard meteorological measurements included solar radiation, air temperature and humidity (HMP45C, Vaisala Inc., Woburn, MA and 10-Plate Gill Radiation Shield, R.M. Young, Traverse City, MI), and both wind speed and direction (Wind Sentry, R.M. Young, Traverse City, MI). In addition, air temperature at 2 m height over the desert was retrieved from the Avdat weather station (Israel Meteorological Service), 1.3 km to the north of the experimental site in the upwind direction. Other measurements included irrigation amounts and leaf area index (LAI2000; Li-Cor Bioscience Inc., Lincoln, NE). Unless otherwise indicated, data were logged at 10 s intervals, and stored as 15 min averages (CR23X and CR5000 dataloggers, Campbell Scientific Inc., Logan, UT).

The components of the energy balance were assessed above the vineyard as well as for both the wet and the dry areas below the vines, which accounted for 14% and 86% of the soil surface respectively (Kool et al., 2016). The assessed energy balance components included R_n, G, H, and LE (all in W m^{-2}; with R$_n$ defined positive when directed towards the surface and all other fluxes are defined positive when directed away from the surface), neglecting energy used for fixation of

carbon dioxide and heat storage in the canopy layer. Vineyard level R_n, (R_{nfield}) was measured 5 m above the soil surface, and R_n below the vines was measured at 0.3 m over the wet (R_{nsWET}) and dry (R_{nsDRY}) soil surface (Q*7, Radiation and Energy Balance Systems, Seattle, WA). G was measured in both the wet (G_{WET}, 1 repetition) and the dry (G_{DRY}, 2 repetitions) area: soil heat flux plates (HFT1.1, Radiation and Energy Balance Systems, Seattle, WA) were buried at 6 cm depth and the heat storage above the plates was determined adjacent to each plate, from measurements of soil water content at 6 cm depth (SDI-12 Soil Moisture Transducer, Acclima Inc., Meridian, ID) and temperature gradients (Soil surface temperature and thermocouples at 1.5, 4.5 and 6 cm depth). Soil surface temperature (T_s) of the wet area (T_{sWET}) and the dry midrow (T_{sDRY}) was measured using infrared thermometers (IRTs) at 0.3 and 2.5 m heights respectively (IRTS-P, field-of-view 28° half angle, Apogee Instruments Inc., Logan, UT). Vineyard-scale turbulent fluxes H_{field} and LE_{field} were measured using an eddy covariance system installed 3.3 m height (CSAT 3-D sonic anemometer, Campbell Scientific Inc., Logan, UT; with an open path infrared gas analyzer, LI-7500, Li-Cor Biosciences Inc., Lincoln, NE). Data were collected at 10 Hz. Post-processing and corrections for calculating half-hourly averages are described by Kool et al. (2016). Additional above-canopy measurements, derived from the eddy covariance flux tower, included air temperature (T_a), wind speed (u_z, m s^{-1}) and friction velocity ($u*$, m s^{-1}). Below the canopy, T_a for the wet area (T_{aWET}) was measured at 0.06 m height using a shielded Beta-Therm thermistor. Diurnal changes in LE_{sWET} were measured on 23 July 2012, using 6 PVC micro-lysimeters (MLs) weighed hourly from before dawn until 2–3 h after sunset (Kool et al., 2014).

2.3. Calculated fluxes

Assuming latent heat from the dry surface was negligible, sensible heat from the dry soil surface (H_{sDRY}) was calculated as

$$H_{sDRY} = R_{nsDRY} - G_{DRY} \tag{2}$$

while H from the wet soil surface (H_{sWET}) was calculated as:

$$H_{sWET} = \rho c_p \frac{T_{sWET} - T_{aWET}}{r_{asWET}} \tag{3}$$

where subscripts DRY and WET refer to the measurements near the dry and wet areas of the soil surface respectively, ρ (kg m^{-3}) is air density, c_p (J kg^{-1} K^{-1}) is air specific heat, and r_{asWET} (s m^{-1}) is resistance to heat transfer between the soil surface and the height of T_{aWET}.

Following Kustas and Norman (1999) and adapted for vineyards by Kool et al. (2016), r_{asWET} was calculated as:

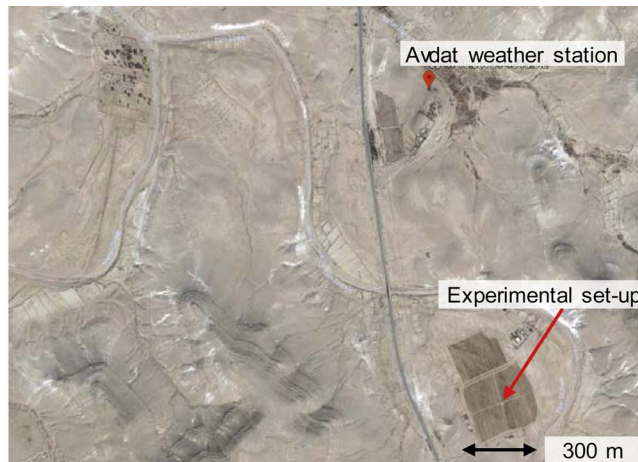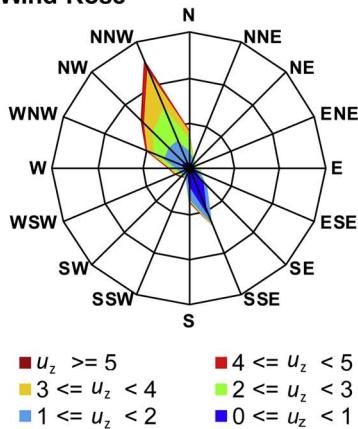$$r_{asWET} = \frac{1}{c(T_{sWET} - T_{aWET})^{1/3} + F_{VA} b u_s} \tag{4}$$

Wind Rose

Fig. 1. Site situation and wind conditions. Wind speed (u_z, m s^{-1}, n = 11,111) from 1 April to 25 July 2012. Image © 2017 DigitalGlobe/Google/ORION-ME, Imagery Date 1 November 2010.

where $c = 0.0025$, F_{VA} is a non-dimensional factor that corrects u_s for the non-continuous nature of the canopy, $b = 0.012$, and u_s (m s^{-1}) is below canopy wind speed computed using equations for continuous canopies (Goudriaan, 1977). Assuming that at a daily scale the canopy architecture affected wind speed over the dry and wet areas in a similar manner, daily F_{VA} was obtained by assuming F_{VA} for r_{asWET} equaled F_{VA} for r_{asDRY}. Replacing H_{sWET}, T_{sWET} and T_{aWET} with H_{sDRY}, T_{sDRY} and T_{aDRY} in Eq. (3) allowed for the determination of r_{asDRY}. This value was entered into Eq. (4) together with T_{sDRY} and T_{aDRY} to determine F_{VA}. The daily average F_{VA} was then used to calculate H_{sWET}.

Kool et al. (2016) found that T_{aDRY} in this system could be estimated using

$$T_{aDRY} = (1 - 0.15 T_{ac}) + 0.15 T_{sDRY} \tag{5}$$

where T_{ac} is the temperature at a reference height in the canopy air space, which can be calculated as:

$$T_{ac} = T_a + \frac{H_{field} u_z}{\rho c_p (u^*)^2} \tag{6}$$

Note that T_{ac} is not the temperature within the canopy volume itself, as the canopy only fills about 20% of the canopy air space above the soil surface. Daily LE from the wet soil surface (LE_{sWET}) was computed as

$$LE_{sWET} = R_{nsWET} - G_{WET} - H_{sWET} \tag{7}$$

Computation of LE_{sWET} at shorter time intervals was not possible, as the wet surface experienced rapid changes with shading, causing de-synchronization between energy balance components measured at slightly different positions/heights. Comparison with ML measurements indicated this approach may result in an underestimation of LE_{sWET} of up to 20% (Kool et al., 2016).

Canopy fluxes were computed as the residual of weighted soil and total vineyard fluxes:

$$R_{nc} = R_{nfield} - (0.86 R_{nsDRY} + 0.14 R_{nsWET}) \tag{8a}$$

$$H_c = H_{field} - (0.86 H_{sDRY} + 0.14 H_{sWET}) \tag{8b}$$

$$LE_c = LE_{field} - 0.14 LE_{sWET} \tag{8c}$$

Because of the limited field-of-view of measured R_{nsDRY} and R_{nsWET}, the diurnal shading patterns across the interrow were not fully captured, limiting R_{nc} calculations to daily values. Conversely, the field-of-views of the IRTs used to compute H_{sDRY} and H_{sWET} were large enough to capture the entire interrow, allowing for hourly estimations of H_c. To determine if the diurnal pattern of LE_c was very different from LE_{field}, the diurnal changes in LE_c were assessed for 23 July 2012, using hourly measurements of LE_{sWET}. This was a well-watered day for a fully grown canopy where the effect of the diurnal pattern of LE_s on LE_{field} was expected to be largest. It was found that reasonable hourly values for LE_c (Fig. 2) could be obtained by assuming:

$$LE_{c.hourly} \cong \frac{LE_{c.daily}}{LE_{field.daily}} LE_{field.hourly} \tag{9}$$

where $LE_{c.daily}$ is obtained from Eq. (8c).

Advection to the wet soil surface (A_{sWET}) was defined as $-H_{sWET}$ for $H_{sWET} < 0$, and the contribution of A_{sWET} to LE_{sWET} was computed as daily A_{sWET}/LE_{sWET}. Advection to the canopy (A_c) was computed as $-H_c$ for $H_c < 0$ and $LE_c > 0$, where $A_c > LE_c$ was forced to $A_c = LE_c$. The contribution of A_c to LE_c was computed as A_c/LE_c. The Priestley Taylor coefficient was computed for both field and canopy energy fluxes ($\alpha_{PTfield}$ and α_{PTc} respectively) using the following equation (Assouline et al., 2016):

$$\alpha_{PT} = \frac{s + \gamma}{\gamma} \frac{LE}{R_n - G} = \frac{s + \gamma}{\gamma} \frac{1}{(1 + \beta)} \tag{10}$$

where β is the Bowen-ratio defined as H_{field}/LE_{field} for $\alpha_{PTfield}$ and H_c/LE_c for α_{PTc}. The ratio $1/(1 + \beta)$ was used rather than $LE/(R_n - G)$ because R_{nc} was not available at hourly time intervals.
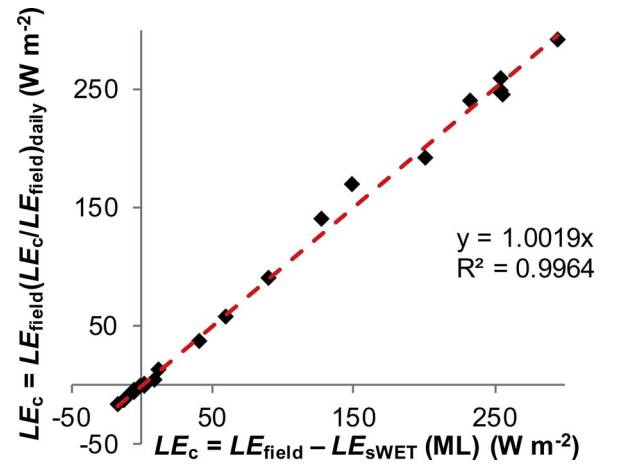

Fig. 2. Hourly canopy latent heat flux (LE_c) for 23 July 2012, calculated from Eq. (8c), where LE_{sWET} is from microlysimeter measurements (ML; x-axis) and calculated from Eq. (9), where daily LE_{sWET} is determined as the residual of the energy balance (Eq. (7)), and hourly LE_c fraction of field LE is assumed to be equal to the daily fraction (y-axis).

2.4. Error analysis

Error analysis included an hourly assessment of energy balance closure at vineyard level. In addition, turbulent fluxes using forced energy balance closure were calculated as

$$LE_{field\beta} = \frac{R_{nfield} - G}{(1 + \beta)} \tag{11}$$

and $H_{field\beta}$ equals $R_{nfield} - G - LE_{field\beta}$. Substituting H_{field} for $H_{field\beta}$ in Eq. (8b) allowed for an assessment of potential errors in H_c caused by energy imbalance. Errors in the relative contribution of advection to LE_c due to possible underestimation of LE_{sWET} and subsequent over-estimation of LE_c was assessed by calculating $A_c/(LE_{field} - 1.2 \times 0.14 LE_{sWET})$ in addition to A_c/LE_c.

3. Results

A seasonal overview of α_{PT} at both field scale and canopy scale for days following an irrigation event provides a rough indication of when advection occurred (Fig. 3a). The irrigation frequency was increased from once a week to twice a week in April, and from twice a week to thrice a week in June. Initial assessment was concentrated on median daytime α_{PT} to reduce the impact of scatter inherent to Bowen-ratio based estimates of α_{PTc}. Throughout the season α_{PTc} values exceeded those of $\alpha_{PTfield}$. Given the drip irrigation system and the large portion of dry soil that is accounted for in $\alpha_{PTfield}$ this is an expected result. The ratio between $\alpha_{PTfield}$ and α_{PTc}, expressed as $\alpha_{PTfield}/\alpha_{PTc}$ increased as the canopy contribution to the overall flux increased and correlated with LAI (Fig. 3b; $R^2 = 0.72$). While $\alpha_{PTfield}$ never exceeded 1.26, α_{PTc} exceeded 1.26 during most of May and July; indicating that advective conditions predominantly occurred during these parts of the growing season.

To explore the factors determining advection, the growing season was divided into three main periods: the first and second periods during which occurrence of advection appeared to be likely (May and July), and the period in between (June). For each period, 21 representative days for which a full dataset existed were selected: 29 April-19 May, 1–9 and 19–30 June, and 1–2 and 6–24 July; hereafter referred to as May, June and July, respectively. The time period prior to 22 April, when there appeared to be no advection, was not further investigated as the canopy was still very small and errors in flux computations were at times larger than the fluxes themselves. Considering that the time of day during which advection occurs can help determine the source of advection, an average day (± standard deviation, n = 21) was
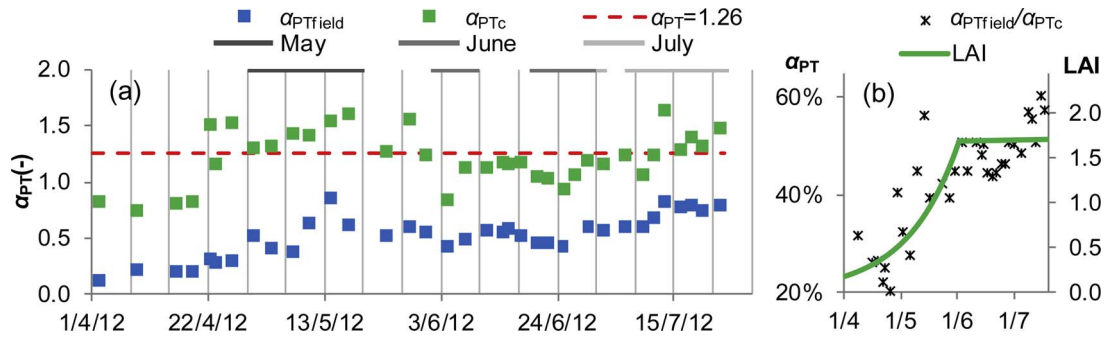
Fig. 3. (a) Daytime median Priestley Taylor coefficient (α_{PT}) values for field and canopy energy fluxes (subscripts field and c respectively) for well-watered days, i.e. 1 day after irrigation. Three-week periods denoted May, June, and July, were identified for further investigation. (b) $\alpha_{PTfield}/\alpha_{PTc}$ compared to leaf area index (LAI).

constructed for each period to form a concentrated presentation of the daily course.

3.1. Advection to the canopy

Average R_{nc} amounted to 6.3 MJ d^{-1} during the May period and 9.0 and 9.1 MJ d^{-1} in June and July respectively and did not vary much with irrigation. An assessment of canopy turbulent fluxes as well as lateral temperature and VPD gradients between the vineyard and the desert, which may be indicative of local advection, is shown in Fig. 4. Each period was further subdivided into average days for 0, 1, and > 1 days after irrigation (DAI), where the sub-period DAI > 1 included hours starting two days after an irrigation event until the next irrigation event.

At the beginning of the season (May) the effect of DAI was minimal with an average LE_c of 180 W m^{-2} around noon, regardless of time from irrigation. For this period, average LE_{field} (2.3 mm d^{-1}) exceeded average irrigation (1.9 mm d^{-1}), indicating a reduction in the amount of water stored in the soil profile. In June, LE_c was 236 W m^{-2} on the first and second days after irrigation (DAI 0 and 1), dropping to a maximum of 136 W m^{-2} at DAI > 1. Average LE_{field} (2.7 mm d^{-1}) still exceeded average irrigation (2.4 mm d^{-1}). In July, LE_c reached 266 W m^{-2} and 182 W m^{-2} on DAI 1 and DAI > 1, respectively, but higher levels of stress caused a delay in the recovery of LE_c following an irrigation event (Fig. 4a–c). At this point in time average LE_{field} (3.2 mm d^{-1}) almost perfectly matched average irrigation (3.3 mm d^{-1}). Similarly, DAI did not affect H_c during the May period, but in June and July H_c was much higher on DAI > 1 than on DAI 0–1 (Fig. 4d–f). Negative H_c, or advection, was observed between 11:00 and 14:00 in May, regardless of DAI, and from 11:00 until 15:00 in July on DAI 1. On DAI 0 in July, advection was limited to 13:00–14:00. Negative H_c was also observed after 18:00 for all three periods but did not appear to contribute to LE_c which was approximately zero from 18:00 and throughout the night (Fig. 4a–c). α_{PTc} was approximately 1.3 at the onset of advection (Fig. 4g-i). As α_{PTc} is dependent on the ratio $LE_c/(H_c + LE_c)$ (Eq. (10)), and both fluxes are small during the night, nighttime α_{PTc} is prone to large errors and was therefore omitted.

Advection to the canopy originated from within or outside the field, where advection from outside the field would have been more likely to occur at higher wind speeds and larger temperature and VPD gradients between the field and the surrounding area. Likewise, soil-to-canopy advection would have been likely to occur at times when the temperature gradient between the soil and the canopy was large. The diurnal courses of lateral air temperature and VPD gradients between the vineyard and the surrounding desert ($\Delta T_{lateral}$ and $\Delta VPD_{lateral}$, respectively) are shown in Fig. 4j–o, where the gradients refer to the air temperature and VPD difference between the vineyard and 1.3 km away from the vineyard. $\Delta T_{lateral}$ appeared to follow a pattern similar to α_{PTc}. The effect of DAI on $\Delta T_{lateral}$ was most marked in July with $\Delta T_{lateral}$ = 0.72 °C at noon on DAI 1, the day of maximum advection,

and 0.15 °C on DAI > 1, when there was no advection. The VPD gradients also indicated a higher potential for local advection on DAI 1 in May and July than in June. The large error bars in both $\Delta T_{lateral}$ and $\Delta VPD_{lateral}$ however, did not allow for conclusive statements regarding local advection.

The average values for u, which could be indicative of local advection, as well as the vertical temperature gradients, which could be indicative of within-field advection, are given in Figs. 5 and 6. As DAI was not found to affect u or the vertical temperature gradients for which measurements were available, the monthly average value for each period is shown. It is likely that DAI affected the temperature near or inside the canopy, but this was not measured. No significant differences were observed in the daily pattern of wind speed between the advective and non-advective periods with maximum wind speed of about 4 m s^{-1} at 17:00 (Fig. 5).

Vertical temperature differences between T_s, T_{ac}, and T_a, showed that during daytime $T_{ac} - T_s < 0$ and $T_{ac} - T_a > 0$, suggesting upward H (Fig. 6). T_a increased from an average daily maximum of 28 °C in May to 32 °C in June and 34 °C in July, while T_{ac} and T_s increased from 30 °C and 44 °C in May to 34 °C and 49 °C in June and 36 °C and 50 °C in July. Peak temperatures of T_a, T_{ac}, and T_s did not occur at the same time of the day, dampening the gradients between the heights.

Advection to the soil surface was assumed to be primarily from the dry soil surface in the midrow to the wet soil surface near the dripline. An assessment for the same three periods showed that small negative H_{sWET} occurred at noon on days with irrigation, ranging between −10 and −30 W m^{-2} (Fig. 7a–c). During these times T_{sWET} was cooler than T_{ac} (Fig. 7d–f). In June and July some advection was also observed one day after irrigation, at 11:00 and 11:00–12:00 respectively. Advection at noon coincided with the time that the temperature contrast between wet and dry soil was largest. At noon the wet strip, located directly underneath the vine-row, was shaded, with average surface temperatures of 28 °C in May, 31 °C in June and 32 °C in July, while the entire dry midrow was sunlit, reaching temperatures of 46 °C, 51 °C and 52 °C in May, June and July respectively.

3.2. Seasonal perspective on the contribution of advection to LE

The daily contribution of advection to LE was determined as the ratio $A_{c,sWET}/LE_{c,sWET}$ for the canopy (subscript c) and the wet soil (subscript sWET) where the daily sum of hourly advection ($\sum_{daily} A_{c,sWET} = \sum_{daily} -H_{c,sWET}$ for $H_{c,sWET} < 0$ and $A_c \le LE_c$) was divided by total daily LE to obtain the mean relative contribution of advection to both LE_c and LE_s (Fig. 8). In addition, daily maximum A_c/LE_c was determined from hourly values. To prevent dividing by a small number, hourly fractions were computed only for LE_c greater than 100 W m^{-2}. Between 22 April and 24 July maximum A_c/LE_c was over 10% in more than half of the days, over 30% in more than a quarter of the days, and over 45% in one decile of the days. On average, A_c accounted for 11% of LE_c or 0.61 MJ d^{-1} from 22 April to 31 May, 2% of
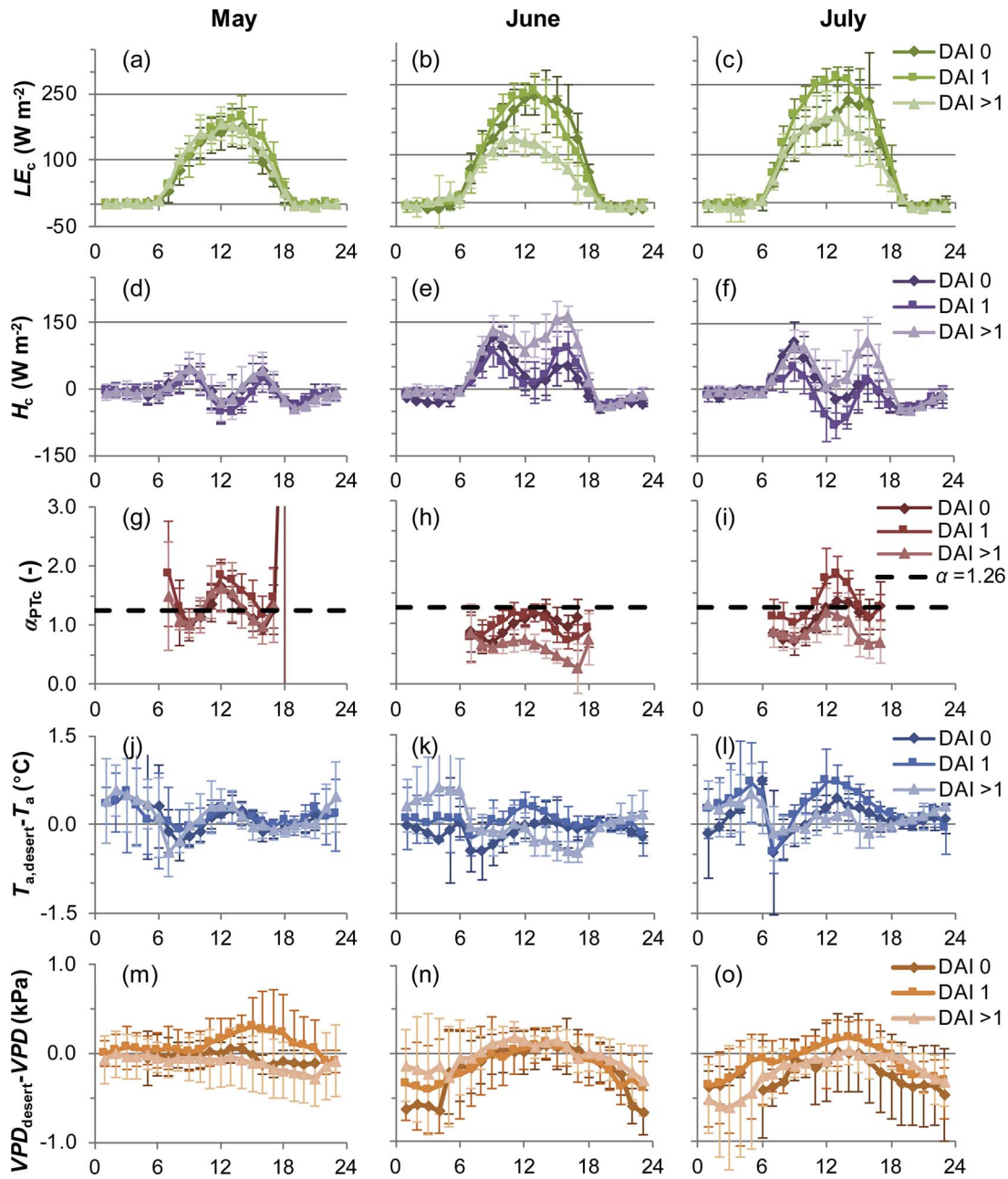
Fig. 4. Average hourly latent heat (LE), sensible heat (H), and computed Priestley-Taylor coefficient (α_{PT}) for the canopy (subscript c), as well as air temperature and VPD difference between the vineyard (T_a, VPD, z = 3.3m) and 1.3 km away from the vineyard ($T_{a,desert}$, VPD_{desert}, z = 2m) for three-week periods in May, June, and July of 2012. Diurnal curves are shown for 0, 1 and > 1 days after irrigation (DAI). Error bars denote the standard deviation (n = 7 on average).
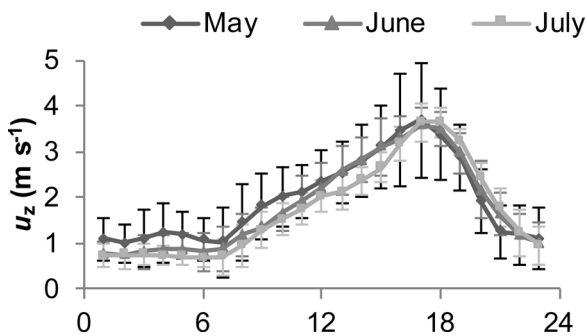

Fig. 5. Average hourly wind speed (u_z) at height z = 3.3 m for three-week periods in May, June, and July of 2012. Error bars denote the standard deviation (n = 21).

LE_c or 0.16 MJ d^{-1} in June, and 11% or 0.78 MJ d^{-1} in July. For the entire observation period A_c was responsible for 8% of LE_c. For the soil, only daily values were available for LE_{sWET}, limiting the analysis of A_{sWET}/LE_{sWET} to daily values. The mean contribution of A_{sWET} to LE_s was 2% for all three periods, with absolute amounts of 0.07, 0.10 and 0.17 MJ d^{-1}, respectively. The increase in A_{sWET} between June and July could largely be attributed to an increase in advection between 17:00 and 19:00.

3.3. Error analysis

Errors due to energy imbalance were most obvious before 10:00 (Fig. 9, July). Energy balance closure ranged from 0.9 to 1.0 between 10:00 and 18:00 and was not significantly altered by irrigation. Results for May and June were similar to July (data not shown). Forced closure
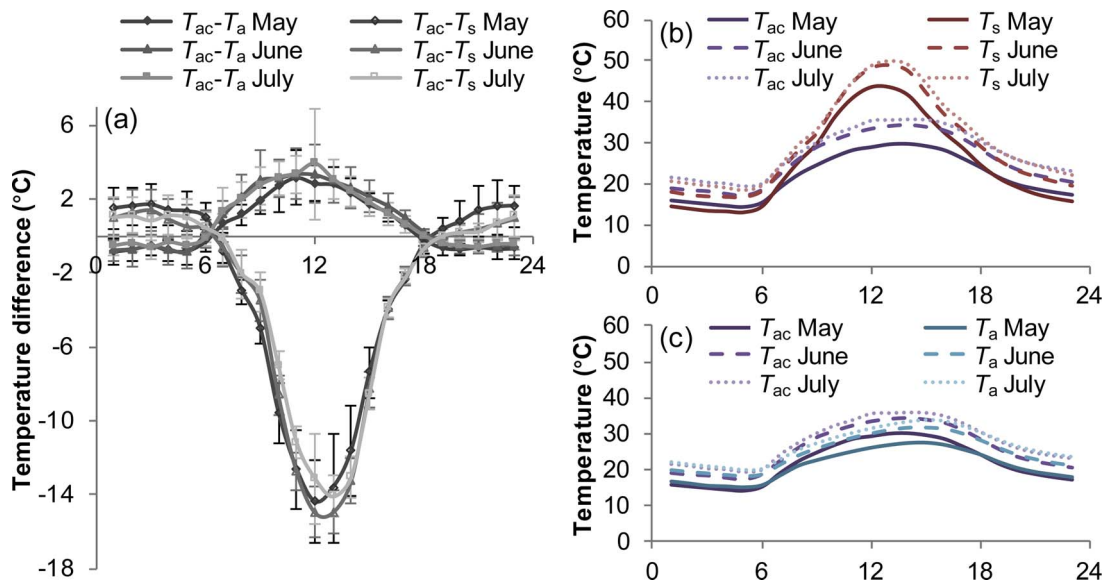
Fig. 6. (a) Average hourly temperature (T) differences between a reference height in the canopy air space (T_{ac}) and 3.3 m height (T_a), as shown in (b), and the soil surface (T_s), as shown in (c), for three week periods in May, June, and July. Error bars denote the standard deviation (n = 21). Advection to the soil surface.

of the energy balance increased the H_c fluxes somewhat (Fig. 10). The overall pattern however, remained unchanged; with advection occurring in May, regardless of irrigation, no advection in June, and stronger advection in July on DAI 1 and sometimes on DAI 0. The average contribution of A_c to LE_c reduced slightly to 7%. Increasing LE_{sWET} by 20% and subsequent decreases in LE_c kept the average contribution of A_c to LE_c at 8%, reducing from 8.1% to 7.9%.

4. Discussion

Initial estimation of α_{PT} for well-watered days proved useful to identify periods of advection, with $\alpha_{PT} > 1.26$ roughly coinciding with periods for which advection was observed (i.e., $H_{field\beta} < 0$). It also gave an immediate indication that advection mostly originated from within-field sources as $\alpha_{PTfield}$ remained low throughout the season (< 1), suggesting that energy from external sources did not contribute to LE_{field}. This indicates that the hot dry surfaces within the field decreased the temperature and VPD gradients between the field and its surroundings (Stoughton et al., 2002) as has been observed in vineyards

elsewhere (Ham et al., 1991; Heilman et al., 1994). Conversely, local advection has been shown to be important in less sparse row crops like cotton and alfalfa (Tolk et al., 2006; Prueger et al., 2012). The ratio between $\alpha_{PTfield}$ and α_{PTc} followed a similar seasonal pattern as LAI for the early and middle part of the season. While no changes were observed in the optical measurements of LAI, the canopy may have continued to become denser towards the end of the season, which may explain why $\alpha_{PTfield}/\alpha_{PTc}$ continued to increase. Another possibility is that the phenological changes towards the end of the season, i.e. the berry ripening, caused an increase in LE_c and thus α_{PTc}. For the three time-periods that were chosen for closer investigation, the canopy was still developing during the advective May period, and fully developed for both the less advective June period and the more advective period in July (Fig. 3). The fully developed canopy also captured more or less the same amount of R_{nc} for the months June and July, while daily R_{nc} was much lower in May.

The reduction in LE_c between well-watered and drier days immediately resulted in a reduction of advection (Fig. 4a–f); indicating advection to the canopy was strongly affected by drought stress.
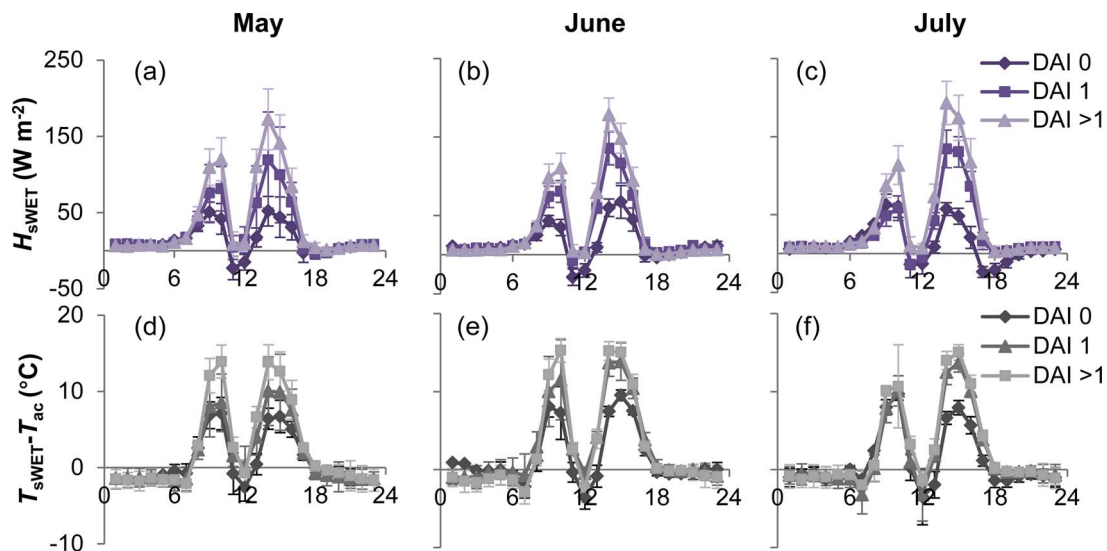

Fig. 7. Average hourly sensible heat (H) and temperature (T) gradients to a reference height in the canopy air space (T_{ac}) for the wet part of the soil surface (subscript sWET) for three-week periods in May, June, and July of 2012. Diurnal curves are shown for 0, 1 and > 1 days after irrigation (DAI). Error bars denote the standard deviation (n = 7 on average).
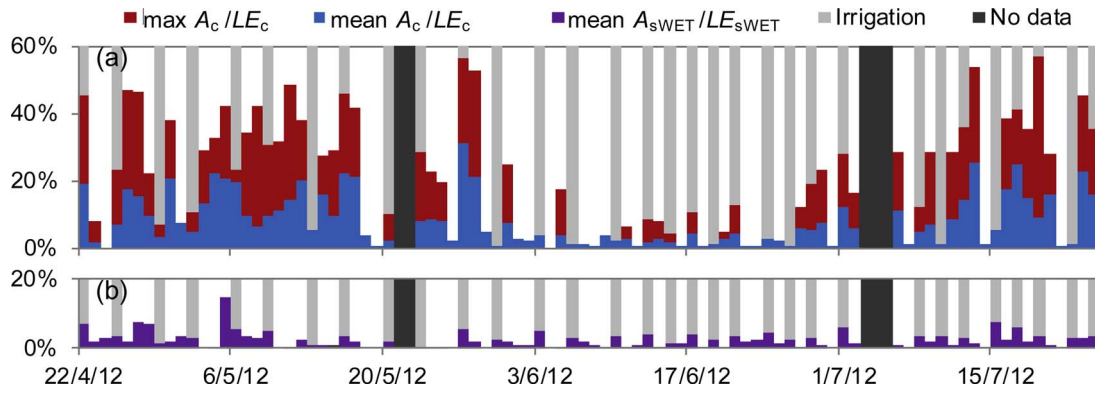
Fig. 8. Daily maximum (max) and mean fraction of latent heat (LE) that can be attributed to advection (A) for the canopy (panel a, subscript c) and the mean fraction of LE that can be attributed to A for the wet soil (panel b, subscript sWET).
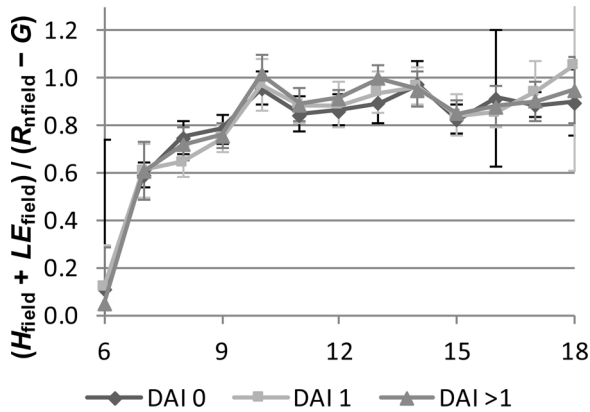

Fig. 9. Average energy balance closure between 6:00 and 18:00 over a three-week period in July 2012, defined as the sum of vineyard (subscript field) sensible and latent heat (H and LE) over the net radiation (R_n) minus soil heat flux (G). Diurnal curves are shown for 0, 1 and > 1 days after irrigation (DAI). Error bars denote the standard deviation (n = 7 on average).

Diurnal patterns show that H_c only dropped below zero for specific hours during the day, and therefore would likely not be noticed when only daily values are considered. H_c was always positive in the morning, declining during mid-day and increasing again right before sunset. Similar initial higher H_c was observed in millet in Burkina Faso, after which H_c dropped below zero and remained negative throughout the day (Lund and Soegaard, 2003). Under advective conditions in a cotton crop in Texas, initial positive H_c only lasted until about 08:00, after which it was strongly negative for most of the day (Ham et al., 1991). A similar diurnal pattern of H_c was observed in a north-south oriented vineyard in Texas, with initial high positive H_c in the morning, negative H_c at midday, and positive H_c in the late afternoon (Heilman et al., 1994). Thus, while positive H_c in the morning appears to be commonplace, the return to positive values in the late afternoon was only reported for vineyards with north-south row orientation. This is an indication that advection in the vineyard mostly originated from the dry midrow, which was fully sunlit around noon but mostly shaded
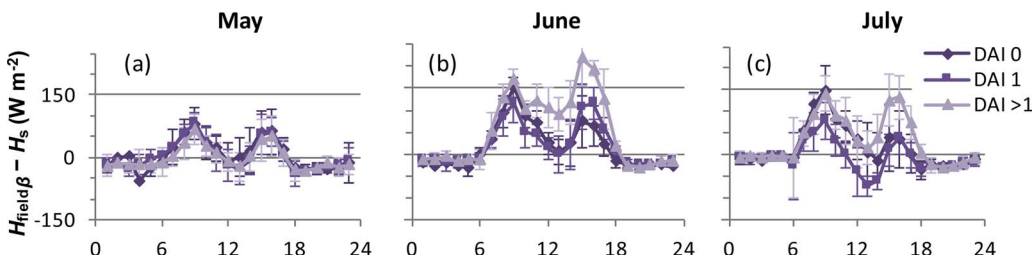
after about 16:00; and not from outside the field, as wind speed only reached its peak around 17:00 (Fig. 3). A study in tomato in a similar environment in the Negev desert suggested that within-row advection was the dominant source of advection during late morning, while local advection became more important in the afternoon (Figuerola and Berliner, 2006). Assessment of α_{PTc} indicated that the traditional value of maximum evaporation without advection of $\alpha_{PT} = 1.2–1.3$, mostly coincided with the point where H_c was about to drop below 0, unlike other studies where $H < 0$ for $\alpha_{PT} > 1.4–1.5$ was observed (Diaz-Espejo et al., 2005; Li and Yu, 2007). While the resemblance of diurnal patterns of α_{PTc} to the gradient in T_a and, to a lesser extent, VPD between the vineyard and the desert does not necessarily indicate local advection, the possibility of local advection cannot be totally ruled out.

Another expected driver of local advection was u_z, however it appeared that u_z remained more or less constant throughout the season, and could not account for differences in advection with time (Fig. 5). Temperature gradients between T_{ac} and T_a and between T_{ac} and T_s did not vary much over the season (Fig. 6). Absolute temperatures increased from May to July, where T_s showed a marked increase from May to June and almost no increase from June to July, while T_a increased steadily by 2 °C each month. These trends resulted in a slightly larger gradient between T_{ac} and T_a in June, when no advection was observed, contrary to the expectation that advection from the soil would be highest when the gradient with the canopy air temperature is largest. Temperature gradients therefore did not appear to be a good indicator for advective time periods, likely because the canopy cover was not large enough to strongly affect T_{ac}. Unlike advection to the canopy, advection to the wet soil was not subject to seasonal change. A slight increase in peak positive H_{sWET} was observed with time (Fig. 7), but did this not appear to affect advective conditions at noon. A_{sWET} predominantly occurred under shaded conditions immediately following irrigation, when temperature contrast to the dry sunlit midrow was sharpest. Figuerola et al. (2013) observed A_{sWET} under similar conditions. As the wet surface was shaded for only a few hours, advective conditions were also limited, contributing very little to the total daily energy balance for the soil surface. Thus, an approach that looks at enhanced evaporation on a daily basis would not detect the contribution of soil-to-soil advection, e.g. the approach of Bonachela et al.

Fig. 10. Average hourly sensible heat (H) for the canopy computed as the difference between vineyard and soil H (subscripts field and s). Forced energy balance closure at vineyard level was used to determine $H_{field\beta}$. Diurnal curves are shown for 0, 1 and > 1 days after irrigation (DAI). Error bars denote the standard deviation (n = 7 on average).

(2001) who determined the daily ratio between evaporation from the wet strip and the theoretical evaporation from a uniformly wetted surface. While there was no evidence that night time advection contributed to LE_c, the contribution of advection between 17:00 and 19:00 in July to LE_{sWET} was confirmed by hourly microlysimeter measurements which showed that LE_{sWET} continued for 2–3 h after sunset (Kool et al., 2014).

The relative fraction A_c to LE_c (Fig. 8a) indicated that A_c contributed significantly to LE_c, even though H_{field} never dropped below zero for $LE_{field} > 0$, confirming that the main source of advection was within-field. That said, the principle source of energy for LE_c was still radiation, as has been emphasized by others (e.g., Ham et al., 1991). Advection on well-watered days was within the same range as the within-field advection contribution of 27–29% of LE_c reported for irrigated sorghum (Hanks et al., 1971), and 32% of LE_c for maize (Zeggaf et al., 2008). The contribution of A_{sWET} to LE_{sWET} was very low (Fig. 8b), this can be attributed to the relatively small fraction of wetted surface in the vineyard, as well as to the limited time that the wet soil surface was shaded each day, with abundantly sufficient available energy for LE_{sWET} during sunlit hours. In two other studies in vineyards experiencing high VPD, large within-field advection was observed in one, which had a North-South orientation (Heilman et al., 1994) while hardly any within-field advection was found in the other, which, however, had and East-West orientation (Yunusa et al., 2004). While these two studies were in very different locations, and there may be other reasons for differences between them, it is possible that advective and non-advective time periods occur at different parts of the growing season, such as found in this study.

The sudden reduction of A_c in June remains somewhat puzzling however. Absence of a similar reduction in A_{sWET} indicates that the explanation has to do with changes in the canopy. Towards the end of June, canopy management included tying and training the canopy close to the trellis and removal of leaves near the developing grape cluster, which would have made the canopy denser and can explain the increase in LE_c while LAI remained the same. Plant size and row density may influence within-field advection in different ways; some suggest that large dense canopies act as a stronger sink for advected heat from the soil (Hicks, 1973), while others suggest a denser canopy will inhibit within-field advection by reducing the fraction of exposed soil (Mitchell et al., 1991). Most likely there is an optimum between these different processes: in both coffee (Gutiérrez and Meinzer, 1994) and millet (Daamen, 1997) the maximum advective enhancement of LE_c was found for intermediate rather than low or high LAI values. The opposite idea, that there is an optimum to minimize advection, was suggested for natural shrub ecosystems, where plant spacing is far enough apart to prevent competition over water, while close enough to minimize within-field advection (Gong et al., 2016).

The observation that between May and June there was a potential decline in A_c, while between June and July all indicators pointed to an increase in A_c is interesting and somewhat surprising. Between May and June, an increase in LAI would have reduced the potential of within-field supply of A_c. This may have been partially offset by the fact that increased LAI and LE_c would have made the canopy a larger sink. However, R_{nc} captured by the canopy also increased, reducing demand for A_c. Between June and July, LAI and R_{nc} remained more or less constant, but LE_c continued to increase, creating a larger sink without decreasing A_c supply. The increase in LE_c might have occurred due to higher leaf density in the canopy, which would not have been captured with optical LAI measurements, or because of changes in stomatal regulation of the vines as a result of phenological changes. The potential supply of A_c from sources outside the vineyard also increased between June and July, as air temperature gradients between the vineyard and the desert increased.

In summary, within field advection varies greatly throughout the season, from periods when there is no advection to periods when advection seems to enhance LE_c by more than 20%. The lack of advection in June seems to indicate that despite an increase in LE_c, the increase in R_{nc} and resulting increase in available energy reduced the energy deficit near the canopy, while the increased LAI reduced the width of the bare interrow exposed to direct solar radiation and thus the potential of within-field advection. In July, the LAI have already stabilized, while both LE_c, and the temperature gradient between the vineyard and the surrounding desert have continued to increase. This allowed for advection to become important again.

5. Conclusion

Advection is often cited as a reason for lack of energy balance closure (Allen et al., 2011) leading to uncertainty in water use estimates. This study suggests that, in addition to within-field advection, local advection may enhance LE_c even when H_{field} remains positive. In this particular vineyard in the Negev desert, distinct periods with and without advection were observed. During advective time periods advection frequently enhanced LE_c by more than 20%. Total advection amounted to an average of about 8% of LE_c over the season, where diurnal patterns suggest that the primary source is within-field advection. This has implications for energy balance based models, which may underestimate transpiration if within-field advection is not considered. Field turbulent fluxes can still be accurately measured under within-field advection, but H_{field} may be underestimated if the source of advection is outside the field. It may be possible to directly measure within-field advection using spectral analysis of eddies, which is already used to differentiate between regional and local advection (Prueger et al., 2012).

The large difference observed between advection in June and July in the current study underlines that small changes in the canopy can have a large impact on advection. This suggests that it may be possible to reduce within-field advection by adopting a more narrow row spacing in, for example, row crops, vineyards and orchards.

References

Alfieri, J.G., Kustas, W.P., Prueger, J.H., Hipps, L.E., Evett, S.R., Basara, J.B., Neale, C.M.U.U., French, A.N., Colaizzi, P., Agam, N., Cosh, M.H., Chavez, J.L., Howell, T.A., 2012. On the discrepancy between eddy covariance and lysimetry-based surface flux measurements under strongly advective conditions. Adv. Water Resour. 50, 62–78. http://dx.doi.org/10.1016/j.advwatres.2012.07.008.

Allen, R.G., Pereira, L.S., Howell, T.A., Jensen, M.E., 2011. Evapotranspiration information reporting: I. Factors governing measurement accuracy. Agric. Water Manage. 98 (6), 899–920. http://dx.doi.org/10.1016/j.agwat.2010.12.015.

Assouline, S., Li, D., Tyler, S., Tanny, J., Cohen, S., Bou-Zeid, E., Parlange, M., Katul, G.G., 2016. On the variability of the Priestley-Taylor coefficient over water bodies. Water Resour. Res. 52 (1), 150–163. http://dx.doi.org/10.1002/2015WR017504.

Blyth, E.M., Harding, R.J., 1995. Application of aggregation models to surface heat flux from the Sahelian tiger bush. Agric. For. Meteorol. 72 (3–4), 213–235. http://dx.doi.org/10.1016/0168-1923(94)02164-F.

Bonachela, S., Orgaz, F., Villalobos, F., Fereres, E., 2001. Soil evaporation from drip-irrigated olive orchards. Irrig. Sci. 20 (2), 65–71. http://dx.doi.org/10.1007/s002710000030.

Bonachela, S., Granados, M.R., López, J.C., Hernández, J., Magán, J.J., Baeza, E.J., Baille, A., 2012. How plastic mulches affect the thermal and radiative microclimate in an unheated low-cost greenhouse. Agric. For. Meteorol. 152 (1), 65–72. http://dx.doi.org/10.1016/j.agrformet.2011.09.006.

Brakke, T.W., Verma, S.B., Rosenberg, N.J., 1978. Local and regional components of sensible heat advection. J. Appl. Meteorol. 17 (7), 955–963. http://dx.doi.org/10.1175/1520-0450(1978)017<0955:LARCOS>2.0.CO;2.

Díaz-Espejo, A., Fernández, J.E., Verhoef, A., Knight, J.R., Villagarcía, L., 2008. The use of high-resolution weighing lysimeters to improve estimates of soil evaporation in drip-irrigated olive orchards. Acta Hortic. 791, 315–320.

Daamen, C.C., 1997. Two source model of surface fluxes for millet fields in Niger. Agric. For. Meteorol. 83, 205–230. http://dx.doi.org/10.1016/S0168-1923(96)02356-8.

Diaz-Espejo, A., Verhoef, A., Knight, R., 2005. Illustration of micro-scale advection using grid-pattern mini-lysimeters. Agric. For. Meteorol. 129 (1–2), 39–52. http://dx.doi.org/10.1016/j.agrformet.2004.12.001.

Eichinger, W.E., Parlange, M.B., Stricker, H., 1996. On the concept of equilibrium evaporation and the value of the Priestley-Taylor coefficient. Water Resour. Res. 32 (1), 161–164. http://dx.doi.org/10.1029/95WR02920.

Figuerola, P.I., Berliner, P.R., 2006. Characteristics of the surface layer above a row crop in the presence of local advection. Atmosfera 19 (2), 75–108.

Figuerola, P.I., Rousseaux, M.C., Searles, P.S., 2013. Soil evaporation beneath and between olive trees in a non-mediterranean climate under two contrasting irrigation

regimes. J. Arid Environ. 97, 182–189. http://dx.doi.org/10.1016/j.jaridenv.2013.07.002.

Gong, J., Jia, X., Zha, T., Wang, B., Kellomäki, S., Peltola, H., 2016. Modeling the effects of plant-interspace heterogeneity on water-energy balances in a semiarid ecosystem. Agric. For. Meteorol. 221, 189–206. http://dx.doi.org/10.1016/j.agrformet.2016.01.144.

Goudriaan, J., 1977. Crop Micrometeorology: A Simulation Study (Simulation Monographs). Pudoc, Center for Agricultural Publishing and Documentation, Wageningen.

Graser, E.A., Verma, S.B., Rosenberg, N.J., 1987. Within-canopy temperature patterns of sorghum at two row spacings. Agric. For. Meteorol. 41 (3–4), 187–205. http://dx.doi.org/10.1016/0168-1923(87)90079-7.

Gutiérrez, M.V., Meinzer, F.C., 1994. Energy balance and latent heat flux partitioning in coffee hedgerows at different stages of canopy development. Agric. For. Meteorol. 68, 173–186. http://dx.doi.org/10.1016/0168-1923(94)90034-5.

Ham, J.M., Heilman, J.L., Lascano, R.J., 1991. Soil and canopy energy balances of a row crop at partial cover. Agron. J. 83 (4), 744–753.

Hanks, R.J., Allen, L.H., Gardner, H.R., 1971. Advection and evapotranspiration of wide-row sorghum in the Central Great Plains. Agron. J. 63 (4), 520–527. http://dx.doi.org/10.2134/agronj1971.00021962006300040002x.

Heilman, J.L., McInnes, K., Savage, M., Gesch, R., Lascano, R.J., 1994. Soil and canopy energy balances in a west Texas vineyard. Agric. For. Meteorol. 71, 99–114. http://dx.doi.org/10.1016/0168-1923(94)90102-3.

Hicks, B.B., 1973. Eddy fluxes over a vineyard. Agric. Meteorol. 12, 203–215. http://dx.doi.org/10.1016/0002-1571(73)90020-4.

Hillel, D., 1998. Environmental Soil Physics. Academic Press, San Diego, CA.

Kool, D., Ben-Gal, A., Agam, N., Šimůnek, J., Heitman, J.L., Sauer, T.J., Lazarovitch, N., 2014. Spatial and diurnal below canopy evaporation in a desert vineyard: measurements and modeling. Water Resour. Res. 50 (8), 7035–7049. http://dx.doi.org/10.1002/2014WR015409.

Kool, D., Kustas, W.P., Ben-Gal, A., Lazarovitch, N., Heitman, J.L., Sauer, T.J., Agam, N., 2016. Energy and evapotranspiration partitioning in a desert vineyard. Agric. For. Meteorol. 218–219, 277–287. http://dx.doi.org/10.1016/j.agrformet.2016.01.002.

Kustas, W.P., Norman, J.M., 1999. Evaluation of soil and vegetation heat flux predictions using a simple two-source model with radiometric temperatures for partial canopy cover. Agric. For. Meteorol. 94, 13–29. http://dx.doi.org/10.1016/S0168-1923(99)00005-2.

Li, L., Yu, Q., 2007. Quantifying the effects of advection on canopy energy budgets and water use efficiency in an irrigated wheat field in the North China Plain. Agric. Water Manage. 89 (1–2), 116–122. http://dx.doi.org/10.1016/j.agwat.2006.12.003.

Lund, M.R., Soegaard, H., 2003. Modelling of evaporation in a sparse millet crop using a two-source model including sensible heat advection within the canopy. J. Hydrol. 280 (1–4), 124–144. http://dx.doi.org/10.1016/S0022-1694(03)00222-1.

McGowan, M., Taylor, H.M., Willingham, J., 1991. Influence of row spacing on growth, light and water use by sorghum. J. Agric. Sci. 116 (3), 329. http://dx.doi.org/10.1017/S002185960007814X.

McNaughton, K.G., Jarvis, P.G., 1983. Predicting effects of vegetation changes on transpiration and evaporation. In: In: Kozlowski, T.T. (Ed.), Water Deficits and Plant Growth, vol. VII. Academic Press, New York, pp. 1–47.

McNaughton, K.G., 1976. Evaporation and advection II: evaporation downwind of a boundary separating regions having different surface resistances and available energies. Q. J. R. Meteorol. Soc. 102 (431), 193–202. http://dx.doi.org/10.1002/qj.49710243116.

Mitchell, P.D., Boland, A.M., Irvine, J.L., Jerie, P.H., 1991. Growth and water use of young, closely planted peach trees. Sci. Hortic. (Amsterdam) 47 (3–4), 283–293. http://dx.doi.org/10.1016/0304-4238(91)90011-M.

Monteith, J.L., 1981. Evaporation and surface temperature. Q. J. R. Meteorol. Soc. 107 (451), 1–27. http://dx.doi.org/10.1002/qj.49710745102.

Oke, T.R., 1987. Boundary Layer Climates, 2nd edition. Taylor & Francis, Abingdon, UK.

Priestley, C.H.B., Taylor, R.J., 1972. On the assessment of surface heat flux and evaporation using large-scale parameters. Mon. Weather Rev. 100 (2), 81–92. http://dx.doi.org/10.1175/1520-0493(1972)100<0081:OTAOSH>2.3.CO;2.

Prueger, J.H., Hipps, L.E., Cooper, D.I., 1996. Evaporation and the development of the local boundary layer over an irrigated surface in an arid region. Agric. For. Meteorol. 78 (3–4), 223–237. http://dx.doi.org/10.1016/0168-1923(95)02234-1.

Prueger, J.H., Alfieri, J.G., Hipps, L.E., Kustas, W.P., Chavez, J.L., Evett, S.R., Anderson, M.C., French, A.N., Neale, C.M.U., McKee, L.G., Hatfield, J.L., Howell, T.A., Agam, N., 2012. Patch scale turbulence over dryland and irrigated surfaces in a semi-arid landscape under advective conditions during BEAREX08. Adv. Water Resour. 50, 106–119. http://dx.doi.org/10.1016/j.advwatres.2012.07.014.

Ringgaard, R., Herbst, M., Friborg, T., 2014. Partitioning forest evapotranspiration: interception evaporation and the impact of canopy structure, local and regional advection. J. Hydrol. 517, 677–690. http://dx.doi.org/10.1016/j.jhydrol.2014.06.007.

Slatyer, R.O., McIlroy, I.C., 1961. Practical Microclimatology. Royal Meteorological Society (Melbourne).

Stoughton, T.E., Miller, D.R., Huddleston, E.W., Ross, J.B., 2002. Evapotranspiration and turbulent transport in an irrigated desert orchard. J. Geophys. Res. 107 (D20), 4425. http://dx.doi.org/10.1029/2001JD001198.

Tolk, J.A., Evett, S.R., Howell, T.A., 2006. Advection influences on evapotranspiration of alfalfa in a semiarid climate. Agron. J. 98 (6), 1646. http://dx.doi.org/10.2134/agronj2006.0031.

Yuge, K., Haraguchi, T., Nakano, Y., Kuroda, M., Anan, M., 2005. Quantification of soil surface evaporation under micro-scale advection in drip-irrigated fields. Paddy Water Environ. 3 (1), 5–12. http://dx.doi.org/10.1007/s10333-004-0058-z.

Yuge, K., Anan, M., Shinogi, Y., 2014. Effects of the micro-scale advection on the soil water movement in micro-irrigated fields. Irrig. Sci. 32 (2), 159–167. http://dx.doi.org/10.1007/s00271-013-0413-1.

Yunusa, I.A.M., Walker, R.R., Lu, P., 2004. Evapotranspiration components from energy balance, sapflow and microlysimetry techniques for an irrigated vineyard in inland Australia. Agric. For. Meteorol. 127 (1–2), 93–107. http://dx.doi.org/10.1016/j.agrformet.2004.07.001.

Zeggaf, A.T., Takeuchi, S., Dehghanisanij, H., Anyoji, H., Yano, T., 2008. A Bowen ratio technique for partitioning energy fluxes between maize transpiration and soil surface evaporation. Agron. J. 100 (4), 988–996. http://dx.doi.org/10.2134/agronj2007.0201.

Zermeño-Gonzalez, A., Hipps, L.E., 1997. Downwind evolution of surface fluxes over a vegetated surface during local advection of heat and saturation deficit. J. Hydrol. 192 (1–4), 189–210. http://dx.doi.org/10.1016/S0022-1694(96)03108-3.